Electron–phonon coupling properties in MgB_2 observed by Raman scattering

2008 J. Phys.: Condens. Matter 20 255235

(http://iopscience.iop.org/0953-8984/20/25/255235)

J. Phys.: Condens. Matter **20** (2008) 255235 (6pp) doi:10.1088/0953-8984/20/25/255235

Electron–phonon coupling properties in MgB_2 observed by Raman scattering

W X Li[1,2], Y Li[2], R H Chen[1,2], R Zeng[1], M Y Zhu[2], H M Jin[2] and S X Dou[1,3]

[1] Institute for Superconducting and Electronic Materials, University of Wollongong, Wollongong, NSW 2522, Australia
[2] School of Materials Science and Engineering, Shanghai University, 149 Yanchang Road, Shanghai 200072, People's Republic of China

E-mail: shi@uow.edu.au (S X Dou)

Received 17 March 2008
Published 22 May 2008
Online at stacks.iop.org/JPhysCM/20/255235

Abstract

The influence of sintering temperature on the critical transition temperature, T_c, for MgB_2 superconductor was investigated systematically with the aid of room temperature Raman scattering measurements and Raman spectral fit analysis. The Raman spectra for all samples can be fitted with one phonon peak coming from the E_{2g} mode at the Γ point of the Brillouin zone and two peaks coming from sampling of the phonon density of states (PDOS) due to disorder. The enhanced E_{2g} mode in the Raman spectra with increasing sintering temperature shows gradual strengthening of the electron–phonon coupling (EPC) in MgB_2, which is the reason why the T_c of samples increases with increasing sintering temperature. The strength of electron–E_{2g} coupling is estimated to be about 2.0 ± 0.5, which is larger than the average strength of the coupling of electrons with all the phonon modes, ~1.23. The T_c dependence on the profiles of the PDOS peaks is described using the variation of the peaks' frequencies and linewidths in different samples.

(Some figures in this article are in colour only in the electronic version)

1. Introduction

Due to its critical transition temperature (T_c) of 39 K, which is high for a binary boride [1], the search for a mechanism and high T_c in the Mg–B system has attracted intense scientific interest worldwide [2]. According to band structure calculations [3] revealing two-dimensional (2D) $sp_xp_y(\sigma)$ bands and three-dimensional (3D) $p_z(\pi)$ bands, the mechanism of superconductivity in MgB_2 has been attributed to the two-band model [4]. In this model, it has become generally accepted that the larger gap is associated with the 2D σ bands arising from the boron planes and has a value of $\Delta_\sigma \cong 7.069$ meV, while the 3D π bands have a gap of $\Delta_\pi \cong 2.70$ meV [5]. The electrons in the σ band strongly couple with phonons imprisoned within the honeycombed boron layer while electrons in the π band show weak coupling. The identification of MgB_2 as a phonon-mediated BCS/Eliashberg superconductor with multiple gaps and strong electron–phonon coupling (EPC) [5] has resulted in much research associated with the spectroscopy of this material [6]. The strength and frequency dependence of the EPC is determined by both the electron–phonon spectral density, $\alpha^2(\omega)F(\omega)$, and the bare phonon density of states (PDOS), $F(\omega)$. The detectable phonon parameters in the measurements of the spectral features are the phonon frequency, the linewidth (full width at half maximum, FWHM), and the intensity, which can all be affected by EPC. In particular, the frequency shift and the linewidth variation can record the change of the phonon characteristics. The effects of EPC on the intensity are rarely discussed because of its sensitivity to the measurement parameters.

Owing to the simple hexagonal structure with space group $P6/mmm$, four optical modes at the point of the Brillouin zone are predicted for MgB_2: a silent B_{1g} mode (at 87.1 meV, ~700 cm^{-1}), the E_{2g} Raman mode (at 74.5 meV, ~600 cm^{-1}), and the infrared active E_{1u} (at 40.7 meV, ~330 cm^{-1}) and A_{2u} (at 49.8 meV, ~400 cm^{-1}) modes. During the exploration of the MgB_2 superconductivity, Raman response

[3] Author to whom any correspondence should be addressed.

measurements have contributed greatly to the understanding of the superconducting mechanism because the E_{2g} mode is Raman active and strongly coupled to the electronic conduction σ-bands. The broad peak observed in the Raman spectra of pure MgB_2 around 600 cm^{-1} (width ~300 cm^{-1}) is attributed to this mode [7], which is in agreement with the theoretical results of 515–665 cm^{-1} [8]. The significant broadening of this Raman peak arises mainly from the exceptionally strong EPC of the E_{2g} mode in the partially occupied planar boron σ bands near the Fermi surface [8]. To understand the dependence of the superconductivity on the phonon frequency in MgB_2, Raman spectroscopy was systematically conducted on samples sintered at different temperatures. The T_c variation was explained by the competition between the E_{2g} mode and the other modes reflected in the Raman spectra. Raman response measurements have the benefits of excellent energy resolution, a relatively large penetration depth, the ability to selectively measure different portions of the Fermi surface(s) [9], and, especially in superconductors, the benefit of revealing both the existence of the superconducting gap and its strong coupling to some of the active Raman phonons [10]. The superconducting energy gaps and changes in the phonon line shapes of MgB_2 below T_c have been studied by the Raman response because the pairing gap on the 2D σ bands and the 3D π bands can be observed directly, due to the symmetry dependence of the Raman spectra [11]. In view of these considerations, there is therefore great potential in developing Raman spectroscopy as a characterization tool for MgB_2.

2. Experimental details

Polycrystalline samples of MgB_2 superconductor were synthesized by *in situ* reaction of mixed powders of micron size magnesium (99%) and nanosize amorphous boron (99.99%). The mixtures were ground for 30 min to achieve homogeneity under inert atmosphere in a glove box and pressed into bulks 10 mm in diameter and about 5 mm in thickness, using pressure of ~600 MPa. Then the bulks were sintered in a tube furnace for 30 min at 650 °C, 750 °C, 850 °C, and 950 °C, respectively, and furnace-cooled to room temperature. High purity argon gas flow was maintained throughout the sintering process. The smooth fresh surfaces were prepared carefully for further measurements.

The T_c values were deduced from the curves of resistivity dependence on temperature, $\rho(T)$, which was measured with the four probe method in the temperature range from 20 to 300 K in a physical properties measurement system (PPMS: Quantum Design). The Raman scattering measurements were performed on the fresh surface, using a confocal laser Raman spectrometer (Renishaw inVia Plus with resolution of 1 cm^{-1}) at room temperature. The 514.5 nm (2.41 eV) wavelength Ar^+ laser was used for excitation of the Raman signals with Raman shift ranges from 250 to 1000 cm^{-1}. Several spots were selected on the same sample for collecting the Raman signals in order to eliminate the influence of random orientation of the microcrystals on the intensities of the Raman spectra.

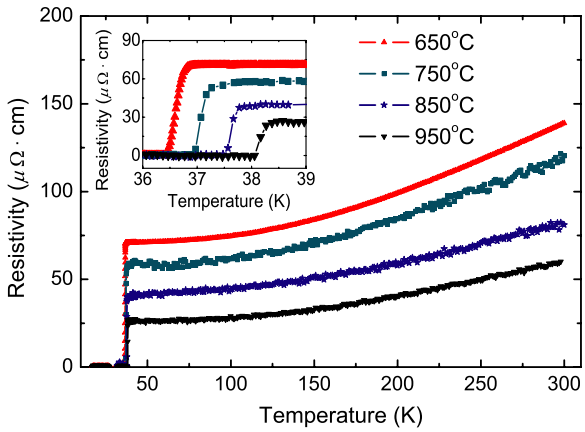

Figure 1. The temperature dependent resistivity $\rho(T)$ curves for MgB_2 sintered at 650, 750, 850, and 950 °C. The inset shows the superconducting transition properties near T_c.

3. Results

The $\rho(T)$ curves for all the samples are plotted in figure 1. Both the ρ(40 K) and the ρ(300 K) are decreased with the enhanced sintering temperature, while the T_c increases gradually from 36.8 to 38.3 K, as shown in the inset of figure 1. Resistivity reflects the electron interaction with high frequency optical phonons, as well as the effect of disorder on each conduction band. Resistivity in MgB_2 reflects the outcome of the scattering process of carriers of σ and π bands with defects (point defects, stacking faults, dislocations, etc), inclusions, and phonons. The resistivity of pure MgB_2 is expressed by the two components from each conduction band, $\rho = \rho_0 + \rho(T)$, with $1/\rho(T) = 1/\rho_\sigma(T) + 1/\rho_\pi(T)$ while ρ_0 is the temperature independent residual resistivity. The temperature dependence of ρ_σ should be larger than that of ρ_π, due to the larger EPC with the E_{2g} optical phonon. Disorder caused by the defects and inclusions depends on the sample processing conditions and influences both the connectivity and the phonon features greatly. The low sintering temperatures lead to imperfect grain growth in polycrystalline MgB_2 and unreacted raw materials become impurities. In particular, oxygen in the atmosphere and the precursor powders is unavoidable for most samples. The high sintering temperature will improve the crystallization and the high crystallinity weakens the scattering effects on electrons. As shown in the following discussion of Raman response results, the σ band has been modified by the high sintering temperature since both the frequency and the linewidth of the E_{2g} mode are strengthened with enhancement of the sintering temperature.

Figure 2 contains the fitted ambient Raman spectra of MgB_2 sintered at 650, 750, 850, and 950 °C for 30 min. There are three fitting peaks in the measurement range from 250 to 1000 cm^{-1}, centered at about 390–410 cm^{-1} (ω_1), 560–580 cm^{-1} (ω_2), and 740–770 cm^{-1} (ω_3), respectively. The MgB_2 spectra were fitted in the range of 250–1000 cm^{-1} by a function used successfully in strongly correlated systems for

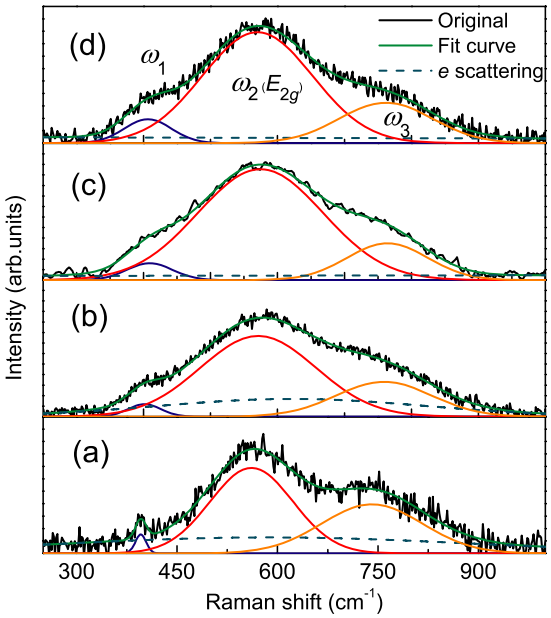

Figure 2. Normalized Raman spectra with fitted E_{2g} mode (ω_2), sampling of PDOS (ω_1 and ω_3 peaks), and electronic scattering background for MgB_2 sintered at 650 °C (a), 750 °C (b), 850 °C (c), and 950 °C (d). The baselines have been subtracted from the patterns.

estimating broad peaks in Raman spectra [12, 13]:

$$S(\omega) = [1 + n(\omega)]\left[\frac{A\omega\Gamma}{\omega^2 + \Gamma^2} + \sum_{i=1}^{N}\frac{A_i\omega\Gamma_i}{(\omega^2 - \omega_i^2)^2 + \omega^2\Gamma_i^2}\right], \quad (1)$$

where the first term represents the low frequency electronic contribution to Raman scattering due to the wide and unstructured electronic background in strongly correlated systems. The sum in the second term accounts for the high frequency contribution to Raman scattering from all three fitted phonon peaks, where ω_i, A_i, and Γ_i are the peak frequency, amplitude, and linewidth, respectively. The quantity $[1 + n(\omega)] = [1 - \exp(-\hbar\omega/k_B T)]^{-1}$ is the Bose–Einstein thermal population factor. The consistency between the experimental data and the fitting curve was quite good in all the investigated samples, as shown in figure 2. The frequencies of the ω_1, ω_2, and ω_3 peaks are in accordance with those observed in the phonon density of states (PDOS) derived from neutron scattering experiments, where different optical contributions have been found around 430, 620, 710, and 780 cm^{-1} [14]. It should be noted that Opel *et al* have derived an alternative expression of equation (1) from a microscopic model, which can be used to pinpoint the relevant parameters for each phonon mode, including a Fano description, and reveal the relationship between the superconductivity and the Raman response in strong coupling superconductors [15]. The strong electron scattering backgrounds in figures 2(a) and (b) are in agreement with the high resistivity in the samples sintered at 650 and 750 °C.

4. Discussion

In the theoretical calculations on the *ab initio* band structure used to describe the EPC between the electronic bands and the E_{2g} mode in MgB_2, the frequency of the E_{2g} mode is in agreement with ω_2 in this study. As for the MgB_2 synthesized at different temperatures, there are a number of defects both in and between the crystals in the samples. Eisterer *et al* have researched the influence of disorder on the superconducting properties of MgB_2 wires and extracted the mean free path of the charge carriers in the σ-band from the Gor'kov–Goodman relation [16]. The wires fall in the range from moderately clean to the dirty limit, and the increase in the upper critical field (H_{c2}) with increasing disorder leads to higher critical currents in high magnetic fields. For disordered systems, relaxation of the q-selection rules may occur, leading to Brillouin zone folding and consequently to the appearance in the Raman spectrum of additional features connected with phonons lying beyond the zone center. In this study, the peaks centered at 390–410 and 740–770 cm^{-1} are understood to arise from sampling of the PDOS due to disorder [8, 17].

The T_c dependence on the fitted peak center values, ω_i, and the linewidth, Γ_i, in the Raman spectra provides a more quantitative description of the effects of the different sintering temperatures. The dependence of the peak center shift $\Delta\omega_i = \omega_{i,T} - \omega_{i,650}$ and the Γ_i on the T_c for the ω_1, ω_2, and ω_3 peaks of all the samples is presented in figure 3, where $\omega_{i,T}$ represents the peak center values of the samples sintered at 650, 750, 850, and 950 °C, respectively. The peak frequencies of ω_1, ω_2, and ω_3 gradually shift to higher energy as T_c increases in the experimental accuracy (±2 cm^{-1}). The frequency of the E_{2g} mode is intimately linked to the quality of the superconductivity of the MgB_2, while the other two modes, especially the ω_3 mode, are responsible for the T_c depression in chemically doped MgB_2 [18].

In order to understand the relationship between the phonon frequency and the T_c, the McMillan formula [19] modified by Allen and Dynes [20] may be used:

$$T_c = \frac{\langle\omega_{\log}\rangle}{1.2}\exp\left(\frac{-1.04(1+\lambda)}{\lambda - \mu^*(1+0.62\lambda)}\right), \quad (2)$$

where $\langle\omega_{\log}\rangle = (690 \times \omega_{E_{2g}}^2 \times 390)^{0.25}$ is the averaged phonon frequency [3], with 690 and 390 cm^{-1} being the phonon frequencies of the other modes in the MgB_2 system (taken from [17]), μ^* is the Coulomb pseudopotential, taken as equal to 0.13 [5], and λ is the EPC constant. For single crystal MgB_2 (T_c = 38 K), λ = 1.29 [5]. Taking these values, the frequency of the fitted $\omega_{E_{2g}}$ = 561, 571, 574, and 570 cm^{-1} gives T_c = 40.6, 40.9, 41.0, and 40.9 K, respectively. The calculated values of T_c are higher than those measured in the experiment for the λ values used in equation (2), as shown in figure 4. These values are consistent with the experimental data, on the assumption that λ is 1.22 for the low T_c sample and 1.24 for the high T_c sample. Although the calculation cannot yield an accurate intensity of the EPC, the results roughly correspond with those obtained via the de Haas–van Alphen effect [21]. It should be noted that T_c depression is observed in high phonon frequency systems for MgB_2 under pressure [7]

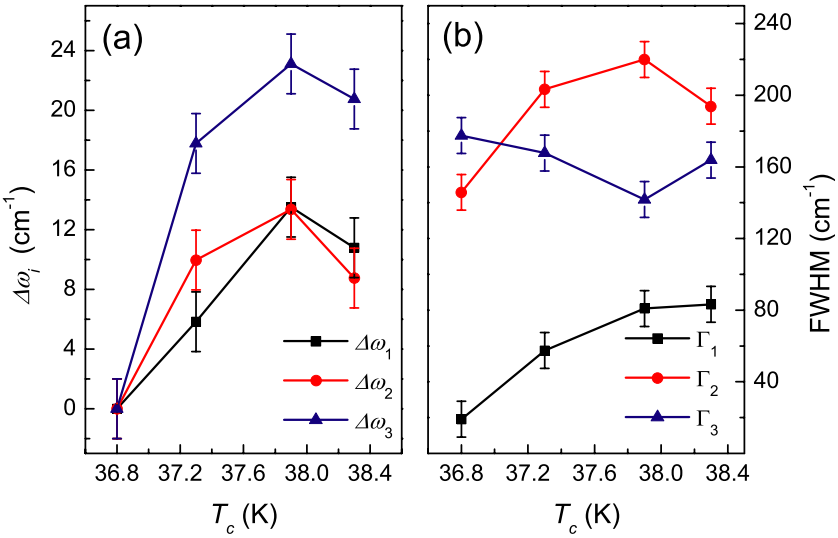

Figure 3. Dependence of the fitted peak center shifts $\Delta\omega_i$ (a) and the fitted linewidths, Γ_i (b) of the ω_1, ω_2, and ω_3 peaks on the superconducting transition temperature for MgB_2 sintered at 650, 750, 850, and 950 °C.

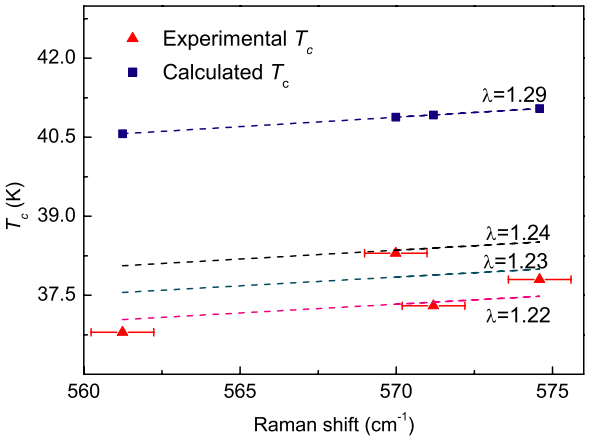

Figure 4. T_c dependence on the Raman shifts of the fitted ω_2 peaks from the McMillan equation calculation and from the experimental values for MgB_2 sintered at 650, 750, 850, and 950 °C. Lines indicate different values of λ to fit the McMillan equation.

and for Al–Ag co-doped MgB_2 [22], which means that the T_c cannot be determined by the phonon frequency alone and that the phonon frequency is just one of the parameters which will influence the T_c performance in MgB_2. The T_c dependence on phonon frequency and unit cell volume has been researched systematically to predict the possibility of high T_c in the chemically doped MgB_2 [23].

As far as the linewidths Γ_i are concerned, as shown in figure 3(b), the low T_c samples show small Γ_1 and Γ_2, but large Γ_3. Γ_1 and Γ_2 increase with the improvement in T_c, while Γ_3 drops quickly. The phonon linewidth is usually believed to be a signal of the intensity of the EPC. Since the E_{2g} mode is considered to be the most relevant phonon in the superconducting transition, the great increase in Γ_2 is related to the T_c improvement, rather than the frequency, as in the above calculation. The large linewidth of the E_{2g} mode has been attributed in previous literature [8, 14] to anharmonic effects, which seems to contradict the trend of the frequency shift in this research. Theoretical calculations performed recently by Calandra *et al* have demonstrated that the Raman data can be explained if dynamical effects beyond the adiabatic Born–Oppenheimer approximation and electron lifetime effects are included in the phonon self-energy, without invoking anharmonicity [24]. This is consistent with later harmonic phonon dispersion results obtained from inelastic x-ray scattering [25]. The variation of Γ_2 for different samples is attributed to the competition between the E_{2g} mode and the other modes. The sample with high T_c has a big Γ_2 (E_{2g}) linewidth, which means a strong EPC. The strength of the EPC for the sample sintered at 850 °C is the greatest, as indicated by its strong E_{2g} mode at a frequency of 574 cm^{-1}, combined with a large linewidth (219 cm^{-1}), and weak disorder Raman response peaks centered at ω_1 = 409 cm^{-1}, with Γ_1 = 81 cm^{-1}, and ω_3 = 764 cm^{-1}, with Γ_3 = 142 cm^{-1}, respectively. Note that these PDOS peaks of the sample sintered at 850 °C are also as prominent as they are because of the short sintering time. Otherwise, they would be folded into the E_{2g} mode. As shown in figures 2(c) and 3 (b), the sample displays PDOS peaks, ω_1 and ω_3, due to defective crystal growth. The electronic background is negligible in the Raman spectra of this sample.

Although the sample sintered at 950 °C should theoretically show a stronger E_{2g} mode than that of any other sample, its crystallinity was degraded by the inevitable evaporation of Mg, due to its high partial pressure when the sintering temperature exceeds 900 °C. Its E_{2g} mode is weakened, while the distortion of its PDOS has become much stronger, as shown in figures 2 and 3. To explain the abnormal behavior, the band scattering effects should be considered. It is believed that T_c values of two- or multiband superconductors are also greatly dependent on the band scattering effects [26]. A practical quantity to evaluate the band scattering effects is the difference in resistivity at the normal state, $\rho(T)$ near T_c, $\rho(T_c)$:

$$\Delta\rho(T) = \rho(T) - \rho(T_c). \tag{3}$$

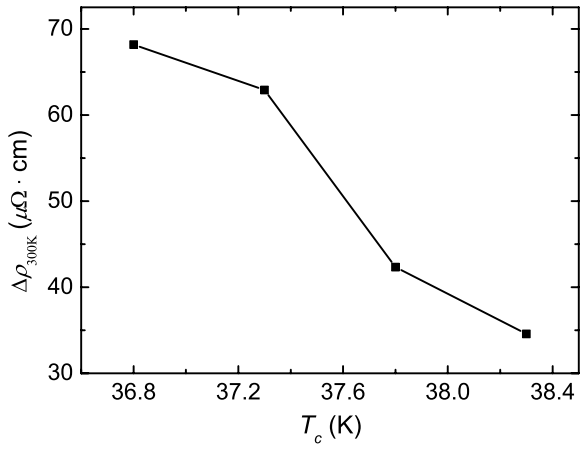

Figure 5. $\Delta\rho$ (300 K) dependence on T_c for MgB_2 sintered at 650, 750, 850, and 950 °C.

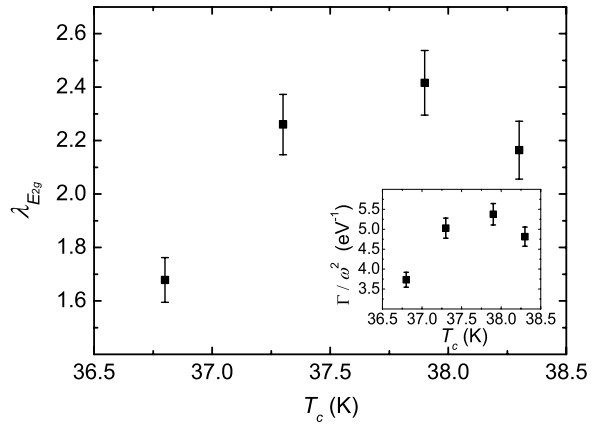

Figure 6. The relationship between the $\lambda_{E_{2g}}$ and T_c obtained by the Allen equation for MgB_2 sintered at 650, 750, 850, and 950 °C. The inset shows the values of Γ_i/ω_i^2 for all the samples.

The $\Delta\rho$ (300 K) for the MgB_2 sintered at 650, 750, 850, and 950 °C are decreased from about 68 to 34 $\mu\Omega$ cm, as shown in figure 5. According to the decreased $\Delta\rho$, the band scattering effects weaken greatly due to the improved crystallinity for the high sintering temperature. The weak band scattering effects compensate the EPC dropping caused by the lattice distortion due to Mg deficiency. The higher T_c observed for the 950 °C sample can be attributed to the combination of moderate EPC and weak band scattering effects. As to the samples sintered at 650 and 750 °C, the weak EPC and remarkable band scattering effects are also responsible for their low T_c values.

Based on the frequency and the linewidth of the E_{2g} mode reflected in the Raman spectra, direct evaluation of the contribution of the E_{2g} mode to EPC is possible for the negligible anharmonic effects in the system. The relationship between the phonon linewidth due to EPC and the phonon coupling constant is given by the Allen equation [27]:

$$\Gamma_2 = 2\pi\lambda_{E_{2g}} N(0)\omega_2^2, \tag{4}$$

where $\lambda_{E_{2g}}$ is the strength of the electron–E_{2g} coupling and $N(0)$ is the density of states (per spin per unit energy per unit cell) on the Fermi surface, and is the only electronic property explicitly occurring in this equation. The measured phonon frequency and phonon linewidth, in the absence of anharmonic contributions, are simply and directly related to the EPC constant, $\lambda_{E_{2g}}$. In pure MgB_2 the total DOS at E_F is taken as $N(0) = 0.354$ states/eV/cell/spin, with the contribution from the σ band being 0.15 states/eV/cell/spin and that from the π band being 0.204 states/eV/cell/spin, respectively [28]. The $N(0)$ is assumed to be constant for small changes of electrons and holes in the pure system. Thus the $\lambda_{E_{2g}}$ for different samples are obtained from equation (4), as shown in figure 6, using the values of Γ_i/ω_i^2 shown in the inset of figure 6 deduced from figure 3. These values are in agreement with 2.5 ± 1.1 obtained for the $q = 0.2\Gamma - A$, E_{2g} mode from inelastic x-ray scattering measurements [25]. The EPC constants of the E_{2g} mode are much larger than the average values, $\lambda = \sim 1.23$, which have been obtained from equation (2). The E_{2g} mode contributes to the strength

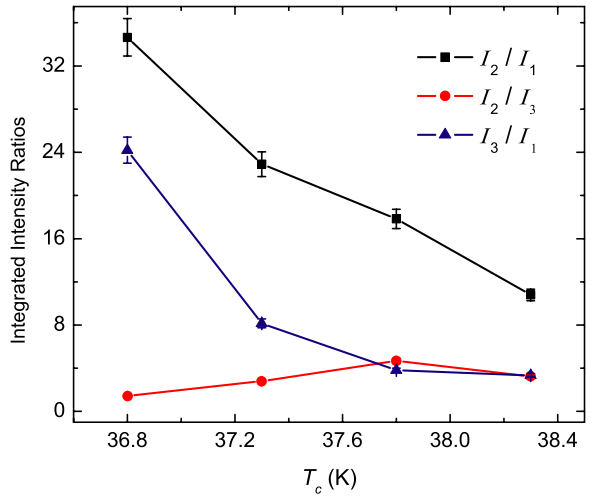

Figure 7. The dependence of the ratios of the integrated intensities of the fitted ω_1, ω_2, and ω_3 peaks on the superconducting transition temperature for MgB_2 sintered at 650, 750, 850, and 950 °C.

of EPC more than any other modes do. It should be noted that the $\lambda_{E_{2g},650}$ of ~1.6 is the smallest one for the largest disorder induced by insufficient crystallization. The high sintering temperature is essential for the improvement of the strength of EPC to be ~2.4. Mialitsin *et al* obtain a value of $\lambda_{E_{2g}}^{\Gamma} \cong 0.3$ [29], which is much smaller than the values in the present work and in [25]. The difference is from their assumption that the remarkable linewidth of E_{2g} is attributed to anharmonicity but not the strong EPC. According to the inelastic x-ray measurements, the anharmonic linewidth is just 1.21 meV (~9.7 cm^{-1}) at 300 K [25], which is much smaller than the Raman measurement results (more than 140 cm^{-1} in this work) [7, 8, 14].

Any comparison of the absolute intensities of different Raman spectra is questionable, due to variations in the measurement parameters, but comparative analysis of the integrated intensities, I_i, has a strong basis. In figure 7, the I_2/I_1, I_2/I_3, and I_3/I_1 ratios are plotted as a function of T_c. As for the two dominant peaks in the Raman spectra, ω_2

and ω_3, their I_2/I_3 values show gradual enhancement as T_c increases. This means that the ω_2 (E_{2g} mode) have become more dominant in the high T_c samples with respect to the ω_1 and ω_3 peaks. The strengthened EPC values due to the enhanced E_{2g} phonon intensity are responsible for the high T_c performance, as indicated by the increased I_2/I_3 ratio. Considering the Γ_3 and I_3 degradation with T_c enhancement, the inhibiting effect of ω_3 peaks on EPC weakens in the high T_c samples. It should be noted that I_2/I_1 and I_3/I_1 decrease sharply in contrast to the increase in T_c, as an indication of the quick development of ω_1 with respect to the growth of ω_2 and ω_3. Although the frequency ω_1, the linewidth Γ_1, and the integrated intensity I_1 all increase with the improvement of T_c, this phonon peak does not contribute to the strengthening of the EPC. On the contrary, it may be responsible for blocking the enhancement of the T_c of MgB_2, because the strengthened ω_1 will indicate disorder in the crystal in a higher T_c sample in a similar way to ω_3 in a lower T_c sample.

5. Conclusion

In summary, the superconducting transition properties of MgB_2 should be partly attributed to the phonon frequencies and linewidths, especially those of the E_{2g} mode deduced from the Raman spectral fit analysis. The strength of the EPC, which is related to the E_{2g} mode, is the dominant factor that will determine the T_c of MgB_2. The specific strength of electron–E_{2g}, $\sim 2.0 \pm 0.5$, is larger than the average strength of the coupling of electrons with all the phonon modes, ~ 1.23. Sampling of the PDOS causes two additional peaks, ω_1 and ω_3, to appear in the Raman spectrum of MgB_2. The presence of the high frequency PDOS peak, ω_3, in the low T_c samples indicates weakening of the EPC strength, while this peak becomes weak in the high T_c samples. At the same time, the low frequency PDOS peak, ω_1, is weak in the low T_c samples and becomes strong for the high T_c samples. The enhanced ω_1 blocks improvement in the EPC intensity, which is necessary to obtain further high T_c in MgB_2.

Acknowledgments

The authors are grateful to Dr T Silver for fruitful discussions. The authors also thank the Australian Research Council, Hyper Tech Research Inc., the China–Australia Government Special Fund for Science and Technology Cooperation (CH060072), the International Cooperation Program of the Science and Technology Committee of Shanghai Municipality (075207036), and the Program for Changjiang Scholars and the Innovative Research Team in the University (IRT0739) for their financial supports.

References

[1] Nagamatsu J, Nakagawa N, Muranaka T, Zenitani Y and Akimitsu J 2001 *Nature* **410** 63
[2] Vinod K, Varghese N and Syamaprasad U 2007 *Supercond. Sci. Technol.* **20** R31
[3] Kortus J, Mazin I I, Belashchenko K D, Antropov V P and Boyer L L 2001 *Phys. Rev. Lett.* **86** 4656
[4] Choi H J, Roundy D, Sun H, Cohen M L and Louie S G 2002 *Nature* **418** 758
[5] Brinkman A, Golubov A A, Rogalla H, Dolgov O V, Kortus J, Kong Y, Jepsen O and Andersen O K 2002 *Phys. Rev.* B **65** 180517(R)
[6] Putti M, Ferdeghini C, Monni M, Pallecchi I, Tarantini C, Manfrinetti P, Palenzona A, Daghero D, Gonnelli R S and Stepanov V A 2005 *Phys. Rev.* B **71** 144505
[7] Goncharov A F, Struzhkin V V, Gregoryanz E, Hu J Z, Hemley R J, Mao H, Lapertot G, Bud'ko S L and Canfield P C 2001 *Phys. Rev.* B **64** 100509(R)
[8] Yildirim T, Gulseren O, Lynn J W, Brown C M, Udovic T J, Huang Q, Rogado N, Regan K A, Hayward M A, Slusky J S, He T, Haas M K, Khalifah P, Inumaru K and Cava R J 2001 *Phys. Rev. Lett.* **87** 037001
[9] Quilty J W, Lee S and Tajima S 2003 *Phys. Rev. Lett.* **90** 207006
[10] Cardona M 1999 *Physica* C **317/318** 30
[11] Devereaux T P and Hackl R 2007 *Rev. Mod. Phys.* **75** 175
[12] Yoon S, Liu H L, Schollerer G, Cooper S L, Han P D, Payne D A, Cheong S W and Fisk Z 1998 *Phys. Rev.* B **58** 2795
[13] Congeduti A, Postorino P, Caramagno E, Nardone M, Kumar A and Sarma D D 2001 *Phys. Rev. Lett.* **86** 1251
[14] Martinho H, Rettori C, Pagliuso P G, Martin A A, Moreno N O and Sarrao J L 2003 *Solid State Commun.* **125** 499
[15] Opel M, Hackl R, Devereaux T P, Virosztek A, Zawadowski A, Erb A, Walker E, Berger H and Forró L 1999 *Phys. Rev.* B **60** 9836
[16] Eisterer M, Müller R, Schöppl K, Weber H W, Soltanian S and Dou S X 2007 *Supercond. Sci. Technol.* **20** S117
[17] Osborn R, Goremychkin E A, Kolesnikov A I and Hinks D G 2001 *Phys. Rev. Lett.* **87** 017005
[18] Postorino P, Congeduti A, Dore P, Nucara A, Bianconi A, Di Castro D, De Negri S and Saccone A 2001 *Phys. Rev.* B **65** 020507(R)
[19] McMillan W L 1968 *Phys. Rev.* **167** 331
[20] Allen P B and Dynes R C 1975 *Phys. Rev.* B **12** 905
[21] Yelland E A, Cooper J R, Carrington A, Hussey N E, Meeson P J, Lee S, Yamamoto A and Tajima S 2002 *Phys. Rev. Lett.* **88** 217002
[22] Shi L, Zhang H R, Zhou S M, Zhao J Y and Zuo J 2006 *J. Appl. Phys.* **100** 023905
[23] Li W X, Li Y, Chen R H, Zeng R, Dou S X, Zhu M Y and Jin H M 2008 *Phys. Rev.* B **77** 094517
[24] Calandra M, Lazzeri M and Mauri F 2007 *Physica* C **456** 38
[25] Shukla A, Calandra M, d'Astuto M, Lazzeri M, Mauri F, Bellin C, Krisch M, Karpinski J, Kazakov S M, Jun J, Daghero D and Parlinski K 2003 *Phys. Rev. Lett.* **90** 095506
[26] Eisterer M 2007 *Supercond. Sci. Technol.* **20** R47
[27] Allen P B 1972 *Phys. Rev.* B **6** 2577
[28] Kortus J, Dolgov O V, Kremer R K and Golubov A A 2005 *Phys. Rev. Lett.* **94** 027002
[29] Mialitsin A, Dennis B S, Zhigadlo N D, Karpinski J and Blumberg G 2007 *Phys. Rev.* B **75** 020509(R)